

# Development of Transition Metal Phosphates NiCoP/NF and Evaluation of Their Hydrogen Evolution Properties

Bo YU, Lei YU\*, Yan LI

*School of Mechanical and Electrical Engineer, Changchun Institute of Technology, Changchun, Jilin, China*

<http://doi.org/10.5755/j02.ms.35415>

*Received 28 October 2023; accepted 8 January 2024*

Energy and the environment are one of the most important global issues in the 21st century. In order to avoid the excessive destruction of the environment and human settlements by fossil fuels, and achieve sustainable development of the Earth, clean energy carrier hydrogen shows its application value. Facing the challenges in preparing transition metal phosphides, in this study, transition metal salts and urea were used as raw materials to react under hydrothermal conditions. The transition metal basic carbonate  $\text{NiCo}_2(\text{CO}_3)_{1.5}\text{OH}_3$  was grown in situ on nickel-foam (NF) substrates. After low-temperature phosphating treatment, NiCoP alloy phosphide electrocatalysts (NiCoP/NF) grown on nickel-foam substrates were obtained. The electrochemical hydrogen evolution performance was tested in 1 mol/L KOH alkaline electrolyte solution. Experiments show, NiCoP/NF heterostructure catalyst has excellent hydrogen evolution performance. In an alkaline medium, the overpotential required to obtain the catalytic current density of  $10 \text{ mA/cm}^2$  is only 93 mV, and the Tafel slope is 118 mV/dec. This is largely due to: 1) the good dispersion of NiCoP/NF nano-catalyst on the Nickel Foam substrate increased the number of active sites exposed; 2) the heterostructure promotes the electron interaction between NiCoP and NF; 3) theoretical calculations show that the construction of NiCoP/NF heterostructure can effectively reduce the dissociation barrier of water, promote the dissociation of water, the kinetic reaction process of electrocatalytic hydrogen evolution is accelerated. Therefore, the construction of NiCoP/NF nanostructured heterogeneous catalysts enriches the application of non-noble metal nanomaterials in the field of hydrogen production from water electrolysis.

**Keywords:** energy problems, transition metal phosphates, catalyst preparation, hydrogen evolution performance evaluation.

## 1. INTRODUCTION

The energy and environmental crisis are a great challenge to human development in the 21<sup>st</sup> century. The design and development of clean and renewable energy and the solution of environmental pollution has become the current research hotspot. With the growing energy crisis and the accompanying global climate change, excessive consumption of traditional fossil fuels (oil, coal, natural gas, etc.), has been unable to satisfy the human development for the energy demand, and the greenhouse gas carbon dioxide and the poisonous gas sulfur and nitrogen oxide released in the process of traditional fuel combustion are seriously endangering the living space of human beings. Therefore, the development of clean energy to replace traditional fossil fuels is an effective means to address the current energy shortage and environmental hazards [1, 2]. Hydrogen is regarded as an ideal substitute for traditional fossil fuels because of its high combustion value and pollution-free combustion products. The world produces about 50 billion cubic metres of hydrogen a year [3], 95 % of hydrogen comes from steam reforming of methane and gasification of coal, by electrolysis of water accounts for only 4 %. Industrial hydrogen production still relies on the conversion of conventional fuels; therefore, it will have potential application value to develop hydrogen production technology by water splitting driven by electricity from clean energy such as solar energy, wind energy and tidal energy.

Electrocatalytic hydrogen evolution (HER) is a half-reaction of electrocatalytic water decomposition, the reaction takes place in an electrolytic cell. The device comprises an electrolyte, a working electrode, a pair electrode, a reference electrode, and an electrochemical workstation. The HER electrocatalysts can be divided into three main groups according to their composition: 1) Pt-based noble metal catalyst; 2) non-noble metal catalyst; 3) Hetero-atom doped catalyst for carbon materials. The first type of catalyst, including Pt, Ru, Rh, Ir, and Pd have been proven to be very efficient HER catalysts, the catalytic effect of Pt is the best. However, the high price and extremely low crust abundance of Pt limit its wide application. In order to develop alternatives to noble metal catalysts, non-noble metals and non-metallic catalysts have been widely studied. The transition metal carbides [4], nitrides [5], phosphates [6, 7], sulfides [8] and hetero-doped carbon materials have been studied extensively. Among them, transition metal phosphates have been widely used in hydrosulfurization, deoxidation and dechlorination because of their Pt-like catalytic activity. Therefore, transition metal phosphates are expected to be an important alternative to noble metals for electrocatalytic hydrogen evolution.

At present, most of the transition metal phosphates electrocatalysts reported in the research exist in the form of powder, and there are many disadvantages in the catalyst powder, for example: poor conductivity, time-consuming electrode preparation process, need additional polymer

\* Corresponding author. Tel: +86-188-4409-6131.  
E-mail: [jd\\_yu@ccit.edu.cn](mailto:jd_yu@ccit.edu.cn) (L. Yu)

binder (nafion solution), electrocatalytic process catalyst powder easy to fall off and excessive dead volume, etc. [9]. It has been shown that an effective strategy to solve the above problems is to grow catalyst arrays on metal substrates in situ, moreover, the new synthesized nano-array structure can effectively solve the problem of catalyst powder characteristics. In this study, transition metal basic carbonate  $\text{NiCo}_2(\text{CO}_3)_{1.5}\text{OH}_3$  nanorod arrays were prepared in situ by hydrothermal reaction of transition metal salts and urea on Nickel Foam (NF) substrate, NiCoP alloy phosphide nanorod array electrocatalyst (NiCoP/NF) was prepared on NF substrate. The results showed that the overpotential of NiCoP/NF was only 93 mV when the current density was  $10 \text{ mA/cm}^2$  in the 1 mol/L KOH potassium hydroxide, and the electrocatalytic activity of NiCoP/NF could be maintained for more than 10 h.

## 2. EXPERIMENT

### 2.1. Reagents and instruments

The list of raw materials for preparing NiCoP/NF and testing its electrocatalytic performance is shown in Table 1.

**Table 1.** List of materials required for the experiment

No.	Name	Suppliers
1	Nickel foam thickness: 0.3 mm	Changsha Liyuan New Materials Co., Ltd.
2	$\text{NiCl}_2 \cdot 6\text{H}_2\text{O}$	Shanghai Aladdin Bio-chemical Technology Co., Ltd.
3	$\text{CoCl}_2 \cdot 6\text{H}_2\text{O}$	Shanghai Aladdin Bio-chemical Technology Co., Ltd.
4	$\text{CH}_4\text{N}_2\text{O}$	Shanghai Aladdin Bio-chemical Technology Co., Ltd.
5	$\text{NaH}_2\text{PO}_2$	Shanghai Aladdin Bio-chemical Technology Co., Ltd.
6	KOH	Shanghai Aladdin Bio-chemical Technology Co., Ltd.
7	Pt/C	Shanghai McLin Biotech Co., Ltd.
8	Ultrapure water	Pall PURELAB TM Plus

In this study, the apparatus for preparing NiCoP/NF and testing its electrocatalytic performance are shown in Table 2.

**Table 2.** List of instruments required for the experiment

No.	Represents the content	Equipment required
1	/Material phase characterization	Rigaku D/max-II B X-ray diffractometer
2	Characterization of material morphology	JEOL JSM 4800F JEOL-2100F
3	XPS	ESCALABMKII spectrometer
4	Electrocatalytic performance test	Chenghua 660 electrochemical workstation

### 2.2. Synthesis of $\text{NiCo}_2(\text{CO}_3)_{1.5}\text{OH}_3$ nanorod arrays

The Nickel Foam was immersed in dilute hydrochloric acid, acetone, and deionized water to remove the oil and oxide layer on the surface, and then the washed NF was cut into  $5 \text{ cm} \times 0.5 \text{ cm}$  for use. Dissolve 0.237 g  $\text{NiCl}_2 \cdot 6\text{H}_2\text{O}$ , 0.474 g  $\text{CoCl}_2 \cdot 6\text{H}_2\text{O}$  and 0.72 g urea in 70 mL distilled water, stir for 30 min, transfer the clarified liquid to a

polytetrafluoroethylene reactor, and place the NF vertically in the reactor. Hydrothermal reaction at  $120^\circ\text{C}$  for 8 h, after cooling, the  $\text{NiCo}_2(\text{CO}_3)_{1.5}\text{OH}_3$  nanorod arrays grown in situ on NF substrate can be obtained.

### 2.3. Synthesis of NiCoP/NF nanorod arrays

Taking sodium hypophosphite as a phosphorus source,  $\text{NiCo}_2(\text{CO}_3)_{1.5}\text{OH}_3$  nanorod arrays and sodium hypophosphite were placed on either side of the combustion boat, and the sodium hypophosphite is upstream of the burning boat, the sodium hypophosphite has a mass of 0.2 g. The tube furnace was then heated to  $350^\circ\text{C}$  under the protection of nitrogen for 2 h. After cooling to room temperature, NiCoP/NF nanorod arrays can be obtained.

### 2.4. HER test

The Chenhua 660 electrochemical workstation was used to test the hydrogen evolution performance of electrocatalyst using a three-electrode system. The catalyst was a working electrode, the carbon rod acted as a pair of electrodes, and the saturated calomel electrode was used as a reference electrode.

The electrolyte was 1 mol/L potassium hydroxide solution (KOH, pH = 14), covering the working electrode with an acrylate adhesive, only the terminal  $0.1 \text{ cm}^2$  region was left as the electrocatalytic test region, and the scanning speed of the polarization curve was  $1 \text{ mV} \cdot \text{s}^{-1}$ .

The electrochemical active area was determined by measuring the cyclic voltammetric curves of the catalysts at different sweep velocities in the non-Faraday region, at a fixed potential ( $-0.75 \text{ V}$  vs RHE), plotting current density difference between sweep speed and fixed potential, by comparing the slope of different catalyst curves, to compare the electrochemical activity area of each catalyst.

The electrochemical impedance testing was performed at potential  $-1.3 \text{ V}$  vs RHE. The test frequency is  $100 \text{ kHz} \sim 0.1 \text{ Hz}$ .

The double-layer capacitance calculation method was applied: 1) the cyclic voltammetric curves of the catalysts in the non-faraday region were measured at different sweep velocities; 2) calculating the current density of  $-0.75 \text{ V}$  anode and cathode; 3) current density difference-sweep velocity curves at different sweep speeds, and the slope of the curve is the double layer capacitance  $C_{dl}$ .

## 3. RESULTS AND ANALYSIS

### 3.1. XRD analysis

In order to study the phase structure information of new catalysts, it was tested by X-ray diffraction analyzer. The XRD patterns of  $\text{NiCo}_2(\text{CO}_3)_{1.5}\text{OH}_3$  nanorods and NiCoP/NF nanorods are shown in Fig. 1. As can be seen from the XRD patterns of Fig. 1 a and b, there are three strong diffraction peaks at  $2\theta = 44.9^\circ$ ,  $52.1^\circ$  and  $76.6^\circ$ . In the curve shown in Fig. 1 a, the diffraction peaks of the nanorods prepared by hydrothermal method are  $2\theta = 17.8^\circ$ ,  $26.7^\circ$ ,  $30.5^\circ$ ,  $33.8^\circ$ ,  $35.6^\circ$ ,  $36.5^\circ$ ,  $39.5^\circ$ ,  $47.4^\circ$ ,  $60.0^\circ$ . The diffraction peaks correspond to the crystal planes of  $\text{NiCo}_2(\text{CO}_3)_{1.5}\text{OH}_3$  respectively (020), (220), (300), (221), (040), (301), (231), (340) and (412), (JCPDS Num: 48-0083). The results show that  $\text{NiCo}_2(\text{CO}_3)_{1.5}\text{OH}_3$  has been successfully prepared. However, due to the repeated

utilization of the material structure or the non-removal of adsorption, the crystal surface appears fuzzy, making the crystal face appear blurry, which results in a strength curve of  $2\theta = (10^\circ - 20^\circ)$ . In the curve shown in Fig. 1 b, the diffraction peak of the phosphating product is  $2\theta = 40.9^\circ$ , the (111) crystal plane corresponding to NiCoP (JCPDS Num: 71-2336) [10], the results show that NiCoP/NF bimetallic phosphates have been successfully prepared.

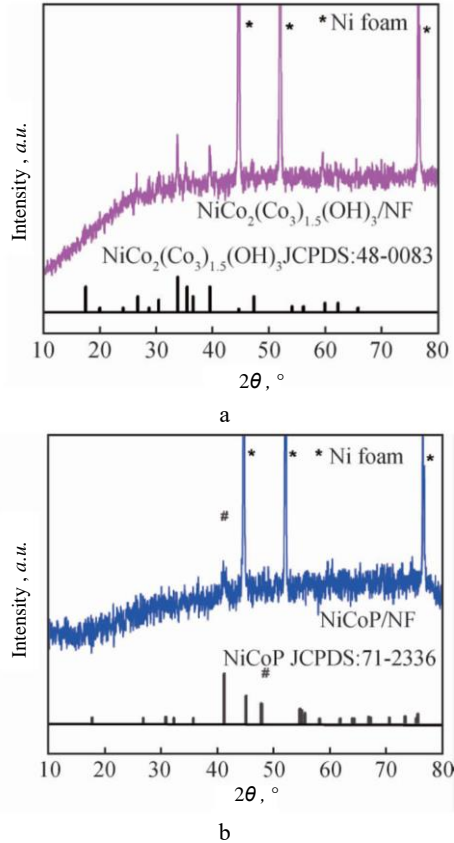


**Fig. 1.** XRD pattern: a–XRD patterns of  $\text{NiCo}_2(\text{CO}_3)_{1.5}\text{OH}_3$  nanorod; b–XRD patterns of NiCoP/NF nanorod

### 3.2. Morphology analysis

To further study the surface distribution of the new catalyst, the Scanning electron microscope of JEOL JSM 4800F and JEOL-2100F were used transmission electron microscope. Fig. 2 shows the characterization characteristics of the new catalyst.

As shown in Fig. 2 a and b, the  $\text{NiCo}_2(\text{CO}_3)_{1.5}\text{OH}_3$  nanorods are uniformly grown on nickel foam after a hydrothermal reaction, the NiCoP/NF formed by phosphating still retained the  $\text{NiCo}_2(\text{CO}_3)_{1.5}\text{OH}_3$  nanorod array morphology. The nanorod array structure is beneficial to increasing the specific surface area of the catalyst and thus fully exposing the active site, and it's good for accelerating mass transfer and charge transfer, thus, the electrocatalytic activity is enhanced.

Fig. 2 c and d are transmission electron microscopy and high-resolution transmission electron microscopy of NiCoP/NF. The lattice diffraction fringes show that the crystal plane spacing is 0.22 nm, corresponding to the NiCoP (111) crystal plane, this result is consistent with the XRD, the existence of NiCoP crystal phase, NF crystal phase and heterostructure was also confirmed.

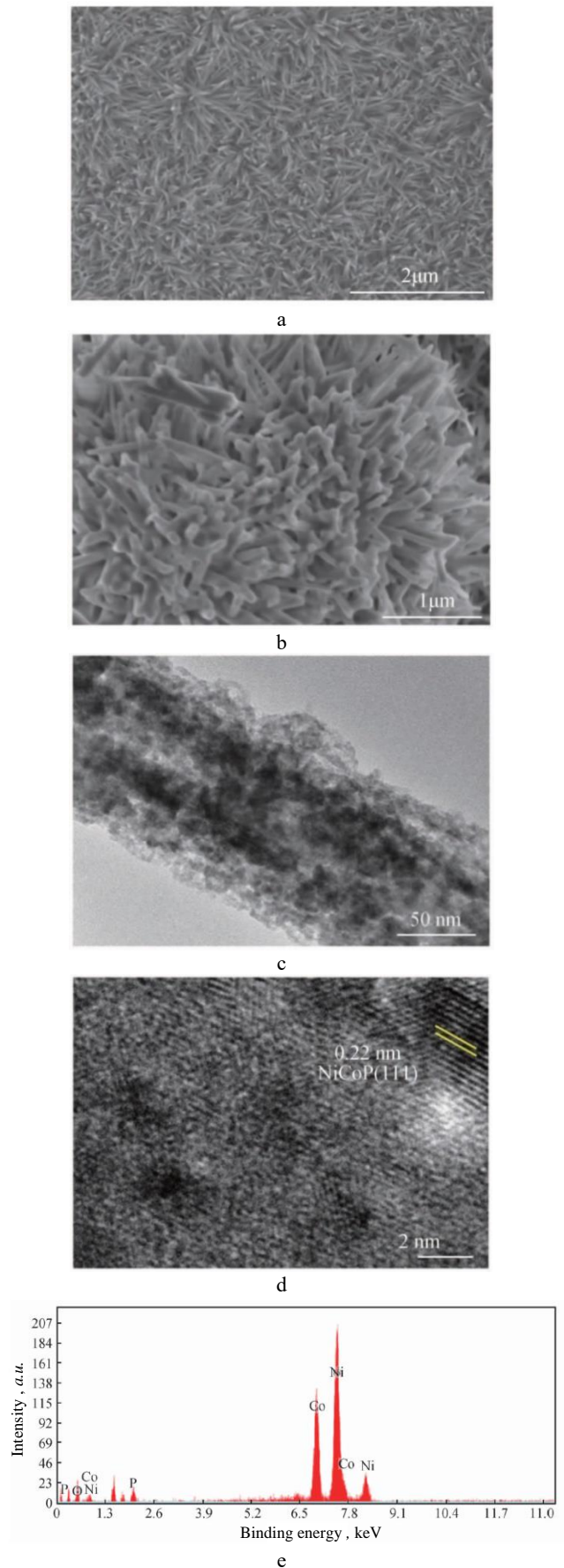


**Fig. 2.** Morphology characteristics of the prepared materials: a–SEM image of  $\text{NiCo}_2(\text{CO}_3)_{1.5}\text{OH}_3$ ; b–SEM image of NiCoP/NF nanorod; c–TEM image of NiCoP/NF nanorod; d–HRTEM image of NiCoP/NF nanorod

Fig. 2 e shows the EDS energy spectrum of NiCoP/NF. The results further confirm the existence of Ni, Co and non-metallic P, O elements, and NiCoP/NF that is mainly distributed in the junction of heterogeneous structure.

Table 3 shows the doping concentration data of Ni, Co, P and O atoms in NiCoP/NF determined by XPS and EDS, because XPS can only measure elements on the surface of a material, and EDS can determine the elements of the material as a whole. However, Ni, Co and P were found to be enriched on the surface of NiCoP/NF. Therefore, concentrations defined by XPS were higher than ones in EDS.

**Table 3.** The doping concentration of Ni, Co and P atoms

No.	Element	XPS	EDS
1	Ni	5.02 %	2.12
2	Co	4.86 %	2.01
3	P	4.57 %	1.53

### 3.3. XPS analysis

The electrochemical reaction takes place mainly on the surface of the catalyst, and the chemical composition and electronic structure of the catalyst surface can be analyzed by X-ray photoelectron spectroscopy (XPS). The results of the analysis are shown in Fig. 3. The full spectrum of XPS photoelectron energy is shown in Fig. 3 a. The peaks of Ni, Co, P and O can be observed, and the existence of Ni, Co, P and O elements is confirmed, which is consistent with the EDS analysis shown in Fig. 2 e.

As shown in Fig. 3 b, in the high resolution XPS map of Ni 2p, there are 6 characteristic peaks after fitting, the binding energy at the 856.2 eV peak corresponds to the positively charged nickel species ( $\text{Ni}^{\delta+}$ ) in the Ni 2p<sub>3/2</sub> orbital, the binding energy peak at 873.8 eV corresponds to the positively charged nickel species ( $\text{Ni}^{\delta+}$ ) in the Ni 2p<sub>1/2</sub> orbital, the peaks with binding energies of 862.2 eV and 879.7 eV belong to the orbit characteristic satellite peak [11], and the binding energy is at 852.3 eV and 870.7 eV belong to  $\text{Ni}^{2+}$  peaks of  $\text{Ni}_x\text{P}_y$  surface after oxidation.

As shown in Fig. 3 c, in the Co 2p high resolution XPS map, there are 6 characteristic peaks after fitting, the peak of binding energy at 778.1 eV and 797.2 eV belong to Co 2p<sub>3/2</sub> and Co 2p<sub>1/2</sub> orbitals, respectively, both correspond to the Co-P bond, the spectral peaks with combined energies of 787.1 eV and 801.2 eV belong to the orbit characteristic satellite peaks, the binding energy at 782.1 eV and 793.2 eV corresponds to Co-O bond [12].

As shown in Fig. 3 d, in the high-resolution XPS map of P 2p, the peak of binding energy at 129.2 eV was attributed to the negatively charged phosphorus species ( $\text{P}^{\delta-}$ ), this is M-P chemical bond (M stands for metal), the peak of binding energy at 133.5 eV was attributed to the water molecules adsorbed on the surface and some phosphorous compounds formed by air oxidation. Therefore, there is an obvious electron interaction between NiCoP and NF component, the NiCoP/NF heterostructure catalysts promote electron transfer, so there's a lot of negative charge around the P atom, this is helpful to the adsorption of  $\text{H}^+$  on the surface of the material in the process of electrolytic hydrogen evolution from water, the overall electrocatalytic performance of the material is further enhanced.

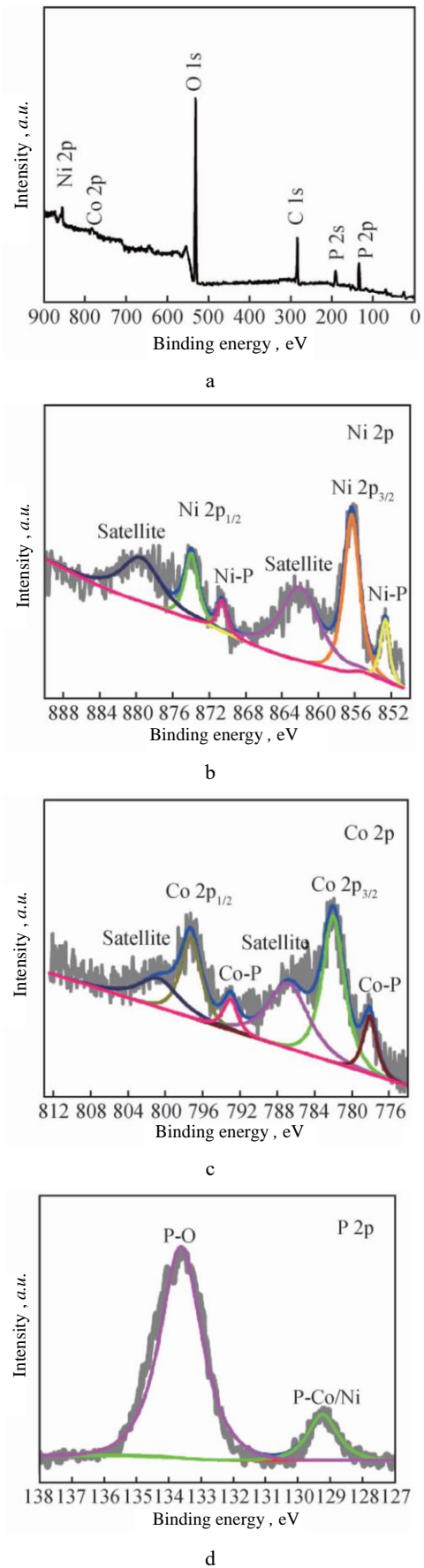


**Fig. 3.** Photoelectron spectra of materials: a – XPS spectrum of NiCoP/NF nanorod; b – HR-XPS spectrum of Ni 2p; c – HR-XPS spectrum of Co 2p; d – HR-XPS spectrum of P 2p

### 3.4. HER evaluation

Using the Chenghua 660 model electrochemical workstation, combined with a three-electrode system, the performance of HER was tested under the condition of alkaline (1.0 mol/L, KOH, pH = 14), and the electrochemical properties of Pt/C electrode were compared under the same conditions. Linear voltammetric curves, TAFIR curves, Nyquist curves and chronopotentiometric curves were used to evaluate the activity and stability of electrocatalytic hydrogen evolution.

#### 3.4.1. Linear scanning curve analysis

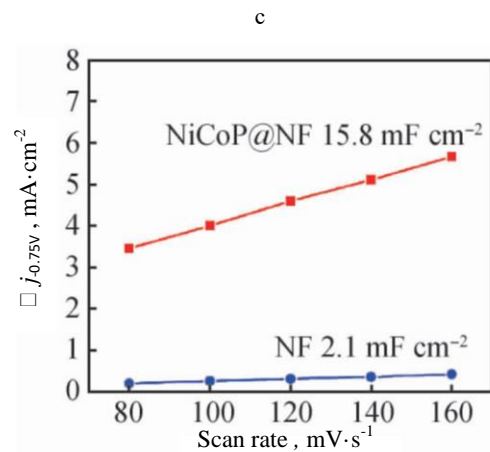
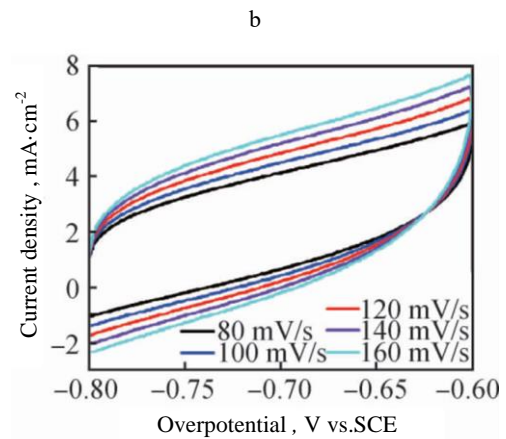
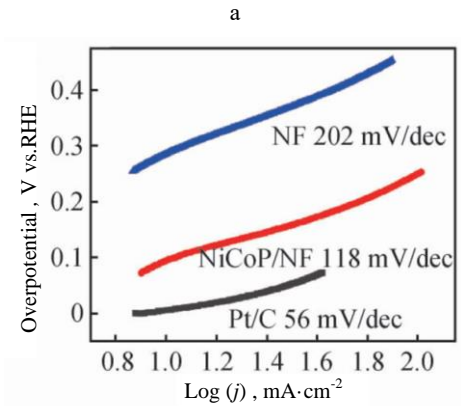
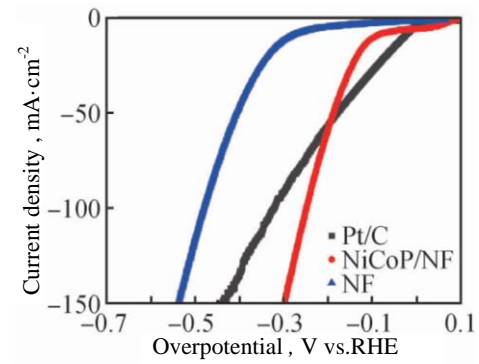
Fig. 4 a shows the linear scan curves for Pt/C, NiCoP/NF and nickel foam and the corresponding overpotential at 10 mA/cm<sup>2</sup> current density. At lower current densities (less than 60 mA/cm<sup>2</sup>), the Pt/C has the highest electrocatalytic activity for hydrogen evolution, the current density of 10 mA/cm<sup>2</sup> can be achieved by an overpotential of 26 mV only. For NiCoP/NF and nickel foam to reach the same current density, the overpotential is 93 mV and 283 mV, NiCoP/NF has higher catalytic activity than nickel foam, and its activity is close to the noble metal Pt/C. As the potential increases, the current density of NiCoP/NF increases rapidly and exceeds that of the noble metal Pt/C, the NiCoP/NF is expected to replace noble metals as catalysts for electrocatalytic hydrogen evolution. At the same time, the overpotential of the catalyst synthesized by other elements is compared when the current density is 10 mA/cm<sup>2</sup> under the same experimental conditions, the specific data are shown in Table 4, it is further proved that NiCoP/NF has remarkable catalytic activity for hydrogen evolution without other impurities.

**Table 4.** Comparison of HER activity under basicity condition

No.	Name	Current density, mA/cm <sup>2</sup>	Overpotential, mV	References
1	NiCoP/NF	10	93	this research
2	Co-VOx-P	10	98	[13]
3	CoP <sub>3</sub> /CoMoP	10	110	[14]
4	CoN/MoC/NMCNFs	10	92.5	[15]

#### 3.4.2. Tafel slope analysis

The Tafel slope provides information about the reaction path and how is fast the chemical kinetics. In an alkaline medium, the mechanism of hydrogen evolution from electrolytic water is as follows: 1) the Volmer reaction between H<sub>2</sub>O and the active site of the catalyst produced H\* (H<sub>2</sub>O + e<sup>-</sup> → H<sub>ads</sub> + OH<sup>-</sup>); 2) hydrogen was precipitated by Heyrovsky step (H<sub>ads</sub> + H<sub>2</sub>O + e<sup>-</sup> → H<sub>2</sub> + OH<sup>-</sup>) or Tafel reaction (2H<sub>ads</sub> → H<sub>2</sub>). Fig. 4 b shows the Tafel slope of Pt/C, NiCoP/NF and NF, as can be seen from the picture, the Tafel slopes of Pt/C, NiCoP/NF and NF are 56 mV/dec, 118 mV/dec and 202 mV/dec, the Tafel slope of NiCoP/NF is lower than that of NF, this shows that NiCoP/NF has a faster rate of electrocatalytic hydrogen evolution. The Tafel slope of 1118 mV/dec indicates that the hydrogen evolution process follows the Volmer-Heyrovsky mechanism [16].



continued on next page

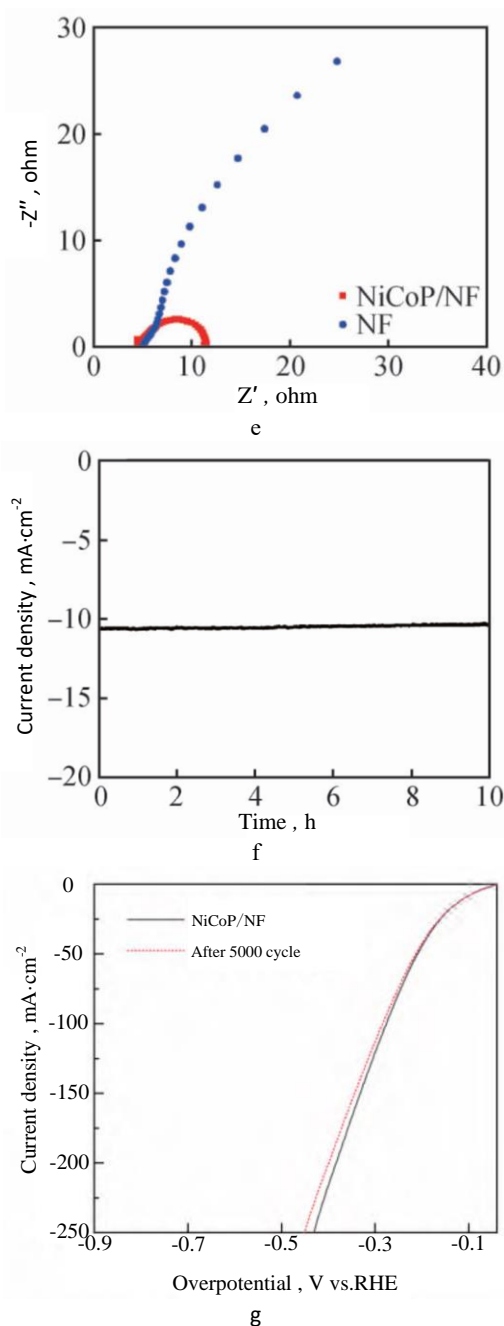


**Fig. 4.** Electrocatalytic hydrogen evolution test: a – LSV curves of Pt/C, NiCoP/NF and NF; b – Tafel slopes of catalysts; c – CV curves of NiCoP/NF at different scan rates; d – the difference in the current density; e – electrochemical impedance spectra (EIS) spectra; f – time dependence of the HER current density curve; g – polarization curves before and after CV test

### 3.4.3. Analysis of active area and catalytic mechanism

The double-layer capacitance ( $C_{dl}$ ) value can represent the size of electrochemical activity specific surface area (ECSAs), therefore, and the  $C_{dl}$  value can be calculated to compare the activity area of the samples. Fig. 4 c shows a CV curve for the voltammetric cycle stability of NiCoP/NF at different sweep speeds, the cyclic voltammetric curves of NiCoP/NF at 80 ~ 160 mV/s scanning rate were measured in the non-Faraday potential range, and the non-Faraday region is (-0.6 ~ -0.8 V vs. RHE). Fig. 4 d shows the current density difference-sweep velocity curve for NiCoP/NF and

nickel foam, the double-layer capacitance  $C_{dl}$  values of NiCoP/NF and nickel foam were calculated respectively at the potential of -0.75 V, the results are 15.8 mF/cm<sup>2</sup> and 2.1 mF/cm<sup>2</sup>, the  $C_{dl}$  of NiCoP/NF is about 7.5 times of that of nickel foam. This indicates that NiCoP/NF has relatively large ECSAs and abundant exposed catalytic active sites, this can be attributed to the abundance of heterostructures in the material, it is advantageous for the catalyst to expose more active sites and to accelerate mass transfer and charge transfer, therefore, the activity of electrocatalytic hydrogen evolution is improved.

### 3.4.4. Electrochemical impedance analysis

In order to further analyze the hydrogen evolution activity of the catalyst, electrochemical impedance spectroscopy (EIS) was used to evaluate the charge transfer ability of catalysts. Fig. 4 e shows NiCoP/NF and Nickel Foam electrochemical impeding Nyquist plot spectra, as you can see from the picture, NiCoP/NF shows a smaller diameter semicircle than Nickel Foam, it has a smaller resistance. This means that NiCoP/NF has a lower charge transfer impedance and is more conductive to electricity. It was beneficial to promote the reaction rate of Volmer and Heyrovsky. In other words, the construction of NiCoP/NF catalyst greatly promotes charge transfer, the resistance of the catalytic electrode is reduced, improved hydrogen chemical kinetics process, this is highly consistent with the XPS results.

### 3.4.5. Electrochemical stability analysis

Stability is another key parameter for the performance evaluation of electrocatalysts. At a current density of 10 mA/cm<sup>2</sup>, the electrochemical stability of the = NiCoP/NF catalytic electrode was studied for 10 h. Fig. 4 f shows the NiCoP/NF stability current density-time curve. In a 10 h potentiostatic test, the current density of NiCoP/NF catalyst is maintained, this proves that NiCoP/NF catalyst has good electrochemical stability. At the same time, the cyclic stability of NiCoP/NF was tested by 5000 voltammetry scans, as shown in Fig. 4 g. There was no significant difference in the LSV curves of the catalysts before and after testing, it is further proved that the catalyst has good electrochemical stability.

## 4. CONCLUSIONS

1. Transition metal phosphates are considered as effective substitutes for Pt like electrocatalytic hydrogen evolution activity. By in situ generation of transition metal basic carbonate  $\text{NiCo}_2(\text{CO}_3)_{1.5}\text{OH}_3$  nanorod arrays on a nickel foam substrate, after low temperature phosphating treatment, the NiCoP alloy phosphide nanorod array electrocatalysts (NiCoP/NF) grown on Nickel Foams were prepared, the preparation and development of a new non-noble metal non-powder electrocatalyst material were completed.
2. Combining characterization techniques, using 1 mol/L KOH solution as a basic electrolyte, based on a 3-electrode electrochemical workstation, the performance of NiCoP/NF electrocatalytic hydrogen evolution was evaluated. In an alkaline medium, the overpotential required to obtain the catalytic current

density of 10 mA/cm<sup>2</sup> is only 93 mV, the Tafel slope is 118 mV/dec, and HER catalytic activity can keep stable for at least 10 h.

3. Representation-based and theoretical computation: 1) NiCoP/NF nanoparticles were uniformly distributed on the surface of nickel foam substrate, the number of active sites exposed was increased ( $C_{dl} = 15.8 \text{ mF/cm}^2$ ), it is beneficial to improve its electrocatalytic hydrogen evolution activity; 2) combined with the XPS results, the existence of heterostructure promotes the electron interaction between NiCoP and NF, the rate of charge transfer and the conductivity of the material are increased; 3) NiCoP/NF heterostructure catalyst can effectively reduce the dissociation barrier of water, greatly facilitates the dissociation of water, it speeds up HER kinetics, furthermore, the hydrogen evolution performance of NiCoP/NF heterostructure nanocatalyst was optimized.
4. The NiCoP/NF heterostructure nanocatalysts were constructed and their performances were evaluated. It provides a theoretical reference for the design of HER electrocatalyst with high activity. The research results have a positive guiding significance for the development of self-supporting electrode catalytic materials for clean energy development in the future, at the same time, it also enriches the application of non-precious metal nanomaterials in the field of hydrogen production from water electrolysis.

## REFERENCES

1. **Schultz, H.** Climate Change and Viticulture: a European Perspective on Climatology, Carbon Dioxide and UV-B Effects *Australian Journal of Grape and Wine Research* 6 (1) 2000: pp. 2–12.  
<https://doi.org/10.1111/j.1755-0238.2000.tb00156.x>
2. **Sutherland, W.J., Bardsley, S., Bennun, L., Clout, M., Côté, I.M., Depledge, M.H., Dicks, L.V., Dobson, A.P., Fellman, L., Fleishman, E., Gibbons, D.W., Impey, A.J., Lawton, J.H., Lickorish, F., Lindenmayer, D.B., Lovejoy, T.E., Nally, R.M., Madgwick, J., Peck, L.S., Pretty, J., Prior, S.V., Redford, K.H., Scharlemann, J.P.W., Spalding, M., Watkinson, A.R.** Horizon Scan of Global Conservation Issues for 2011. *Trends in Ecology & Evolution* 26 (1) 2011: pp. 10–16.  
<https://doi.org/10.1016/j.tree.2010.11.002>
3. **Balat, M.** Potential Importance of Hydrogen as A Future Solution to Environmental and Transportation Problems *International Journal of Hydrogen Energy* 33 (15) 2008: pp. 4013–4029.  
<https://doi.org/10.1016/j.ijhydene.2008.05.047>
4. **Ye, M., Hu, F., Yu, D., Han, S., Peng, S.** Hierarchical FeC/MnO<sub>2</sub> Composite with in-situ Grown CNTs as An Advanced Trifunctional Catalyst for Water Splitting and Metal-Air Batteries *Ceramics International* 47 (13) 2021: pp. 18424–18432.  
<https://doi.org/10.1016/j.ceramint.2021.03.166>
5. **Lin, L.W., Piao, S.Q., Choi, Y.J., Lyu, L.L., Hong, H., Kim, D., Lee, J., Zhang, W., Piao, Y.Z.** Nanostructured Transition Metal Nitrides as Emerging Electrocatalysts for Water Electrolysis: Status and Challenges *Energy Chem* 4 (2) 2022: pp. 100072.  
<https://doi.org/10.1016/j.enchem.2022.100072>
6. **Jiang, N., Shi, S.J., Cui, Y.Y., Jiang, B.L.** Effect of Phosphorization Temperature on the Structure and Hydrogen Evolution Reaction Performance of Nickel Cobalt Phosphide Electrocatalysts *Catalysis Communications* 171 2022: pp. 106507.  
<https://doi.org/10.1016/j.catcom.2022.106507>
7. **Bao, T., Song, L.M., Zhang, S.J.** Synthesis of Carbon Quantum Dot-Doped NiCoP and Enhanced Electrocatalytic Hydrogen Evolution Ability and Mechanism *Chemical Engineering Journal* 351 2018: pp. 189–194.  
<https://doi.org/10.1016/j.cej.2018.06.080>
8. **Han, L., Feng, K., Chen, Z.** Interface Engineering of Self-Supported Electrode for Electrochemical Water splitting *Energy Storage Science and Technology* 11 (6) 2022: pp. 1934–1946.  
<https://doi.org/10.1002/ente.201700108>
9. **Ma, T.Y., Dai, S., Qiao, S.Z.** Self-supported Electrocatalysts for Advanced Energy Conversion Processes *Materials Today* 19 (5) 2016: pp. 265–273.  
<https://doi.org/10.1016/j.mattod.2015.10.012>
10. **Tong, M., Wang, L., Yu, P., Xu, L., Fu, H.** 3D Network Nanostructured Nicop Nanosheets Supported on N-Doped Carbon Coated Ni Foam as A Highly Active Bifunctional Electrocatalyst for Hydrogen and Oxygen Evolution Reactions *Frontiers of Chemical Science and Engineering* 12 (3) 2018: pp. 417–424.  
<https://doi.org/10.1007/s11705-018-1711-1>
11. **Lin, Y., Sun, K., Chen, X., Chen, C., Pan, Y., Li, X., Zhang, J.** High-Precision Regulation Synthesis of Fe-doped Co<sub>2</sub>P Nanorod Bundles as Efficient Electrocatalysts for Hydrogen Evolution in All-pH Range and Seawater *Journal of Energy Chemistry* 55 2021: pp. 92–101.  
<https://doi.org/10.1016/j.jechem.2020.06.073>
12. **Zhou, P., Zhuai, G., Lv, X., Liu, Y.Y., Wang, Z., Wang, P., Zheng, Z., Cheng, H., Dai, Y., Huang, B.** Boosting the Electrocatalytic HER Performance of Ni<sub>3</sub>N-V<sub>2</sub>O<sub>3</sub> via the Interface Coupling Effect *Applied Catalysis B: Environmental* 283 2021: pp. 119590.  
<https://doi.org/10.1016/j.apcatb.2020.119590>
13. **Zhu, Z., Xu, K., Guo, W., Zhang, H., Xiao, X., He, M., Yu, T., Zhao, H., Zhang, D., Yang, T.** Vanadium-phosphorus Incorporation Induced Interfacial Modification on Cobalt Catalyst and Its Super Electrocatalysis for Water Splitting in Alkaline Media *Applied Catalysis B: Environmental* 304 2022: pp. 120985.  
<https://doi.org/10.1016/j.apcatb.2021.120985>
14. **Jiang, D., Xu, Y., Yang, R., Li, D., Peng, S., Chen, M.** CoP<sub>3</sub>/CoMoP Heterogeneous Nanosheet Arrays as Robust Electrocatalyst for pH-Universal Hydrogen Evolution Reaction *ACS Sustainable Chemistry & Engineering* 7 (10) 2019: pp. 9309–9317.  
<https://doi.org/10.1021/acssuschemeng.9b00357>
15. **Wu, W., Zhao, Y., Li, S., He, B., Peng, X., Zhang, J., Wang, G.** P Doped MoS<sub>2</sub> Nanoplates Embedded in Nitrogen Doped Carbon Nanofibers as An Efficient Catalyst for Hydrogen Evolution Reaction *Journal of Colloid and Interface Science* 547 2019: pp. 291–298.  
<https://doi.org/10.1016/j.jcis.2019.04.004>
16. **Lu, A., Chen, Y., Li, H., Dowd, A., Corite, M.B., Xie, Q., Guo, H., Qi, Q., Peng, D.L.** Magnetic Metal Phosphide Nanorods as Effective Hydrogen-Evolution Electrocatalysts *International Journal of Hydrogen Energy* 39 (33) 2014: pp. 18919–18928.  
<https://doi.org/10.1016/j.ijhydene.2014.09.104>

